A novel functional single-cell approach to probing nitrogen-fixing bacteria in soil communities by resonance Raman spectroscopy with $^{15}N_2$ labelling

Li Cui,[†] *Kai Yang,*[†,‡] *Hong-Zhe Li,*[†,‡] *Han Zhang,*[†] *Jian-Qiang Su,*[†] *Maria Paraskevaidi,*[§] *Francis L Martin,*[§] *Bin Ren,*[δ] *Yong-Guan Zhu,*[*,†,θ]

[†]Key Lab of Urban Environment and Health, Institute of Urban Environment, Chinese Academy of Sciences, Xiamen 361021, China. [‡]University of Chinese Academy of Sciences, 19A Yuquan Road, Beijing 100049, China. [θ]State Key Laboratory of Urban and Regional Ecology, Research Center for Eco-Environmental Sciences, Chinese Academy of Sciences, Beijing 100085, China. [§]School of Pharmacy and Biomedical Sciences, University of Central Lancashire, Preston PR1 2HE, UK. [δ]Department of Chemistry, Xiamen University, Xiamen 361005, China.

Li Cui and Kai Yang contributed equally to this work.

TOC/Abstract art

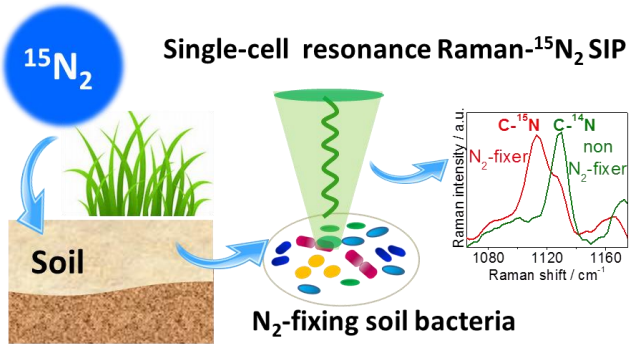

ABSTRACT

Nitrogen (N) fixation is the conversion of inert nitrogen gas (N_2) to bioavailable N essential for all forms of life. N_2-fixing microorganisms (diazotrophs), which play a key role in global N cycling, remain largely obscure because a large majority are uncultured. Direct probing of active diazotrophs in the environment is still a major challenge. Herein, a novel culture-independent single-cell approach combining resonance Raman (RR) spectroscopy with $^{15}N_2$ stable isotope probing (SIP) was developed to discern N_2-fixing bacteria in a complex soil community. Strong RR signals of cytochrome c (Cyt c, frequently present in diverse N_2-fixing bacteria), along with a marked $^{15}N_2$-induced Cyt c band shift, generated a highly distinguishable biomarker for N_2 fixation. $^{15}N_2$-induced shift was consistent well with ^{15}N abundance in cell determined by isotope ratio mass spectroscopy. By applying this biomarker and Raman imaging, N_2-fixing bacteria in both artificial and complex soil communities were discerned and imaged at the single–cell level. The linear band shift of Cyt c *versus* $^{15}N_2$ percentage allowed quantification of N_2 fixation extent of diverse soil bacteria. This single-cell approach will advance the exploration of hitherto uncultured diazotrophs in diverse ecosystems.

Keywords: single-cell resonance Raman, N_2-fixing bacteria, $^{15}N_2$ stable isotope probe, cytochrome c, soil community

INTRODUCTION

Nitrogen (N) is an essential element sustaining all forms of life on Earth. Biological fixation is a critical process converting inert nitrogen gas (N_2) to bioavailable N (ammonia or nitrate) required by all living organisms for biosynthesis. It has been estimated that over half of the fixed N sustaining the world's population is supplied by biological fixation.[1,2] This process is exclusively performed by bacteria and archaea (diazotrophs) in free-living form[3] or in symbiosis with coral,[4] higher plants,[5] or animals in different ecosystems.[6-9] Despite the importance of biological N_2 fixation, active diazotrophs along with their distribution in ecosystems, remain largely unknown.[10,11] One important reason is that a large proportion of diazotrophs remain uncultured to date.

Molecular methods exploiting nitrogenase *nifH* genes have been widely used to evaluate the potential of N_2 fixation in diverse ecosystems in a culture-independent fashion.[9,10,12,13] Microorganisms expressing *nifH* genes, including a large portion of uncultured bacteria, were reported to have the genetic potential for N_2 fixation.[7,10,14] However, discordance between presence or transcription of *nifH* and N_2-fixation activity has been revealed,[12,13] suggesting that species with genetic potential do not necessarily fix N_2. Hence, a functional or phenotypic means of identification of N_2-fixing microorganisms is urgently needed. Stable isotope probing (SIP) with $^{15}N_2$ is reported to be the only direct and unambiguous means for identifying N_2-fixing bacteria and quantifying biological N_2 fixation.[15,16] Combining $^{15}N_2$ SIP with single-cell level characterization provides additional advantages of allowing one to bypass the need for culture, whilst imaging of distribution of N_2-fixation species in complex communities such as bacteria-protist symbionts.[7] $^{15}N_2$-SIP combined with high spatial resolution secondary ion mass spectroscopy (SIMS) - especially

NanoSIMS - is one of the very few available techniques that can probe active N_2-fixing bacteria at the single-cell level.[6,7,10,12,17,18] By applying single-cell NanoSIMS to analyze $^{15}N_2$-incubated sample, a novel cyanobacterial group actively fixing N_2 was discovered in a microbial mat; in contrast, despite expressing genetic potential, a N_2-fixing deltaproteobacteria was excluded due to a lack of ^{15}N enrichment.[10,12] NanoSIMS imaging of an *in vivo* ^{15}N-labeled protist inhabiting wood-eating roach revealed N_2 fixation in bacterial ectosymbionts of protist.[7] These applications advance the exploration of uncultured diazotrophs. Nevertheless, SIMS is a destructive approach and thus does not allow important downstream genomic sequencing or even cultivation of active N_2-fixing cells.

Raman spectroscopy is an attractive non-destructive method capable of providing information about the chemical bonds of various biomolecules of bacteria and discerning functional bacteria at the single-cell level.[19,20] For some cells with specific pigments such as cytochrome c (Cyt c), carotenoids or chlorophyll, strong resonance Raman (RR) signals can be excited if the laser wavelength is within - or close to - the electronic transition of molecules.[21-27] Selective enhancement of RR generates a highly characteristic Raman feature of pigment-containing bacteria. Measurement time can also be greatly reduced, facilitating a relatively rapid spectral acquisition such as Raman imaging. Raman imaging is similar to NanoSIMS imaging by providing information regarding the spatial distribution of bacteria in microbial communities.[21,23] More importantly, in combination with ^{13}C or D_2O-SIP, single-cell Raman or RR can detect functional or active cells in their natural habitat, based on the Raman shift induced by substitution of 'light' atom in a chemical bond by its 'heavier' isotope.[19,28,29] Despite these advantages, ^{15}N-induced shifts are far less distinguishable than ^{13}C or ^{2}D-induced, and the few reports of single-cell Raman

with ^{15}N-SIP were all limited to pure-cultured bacteria.[19,30] Recently, owing to the finding of clear ^{15}N-induced shifts in surface-enhanced Raman spectra (SERS) of bacteria,[19,31] SERS was successfully applied for bulk analysis of N assimilation by environmental bacterial community in a wetland.[31] However, because SERS substrates can easily be contaminated by environmental medium and damaged by laser, single-cell SERS has not been achieved in complex environmental microbial communities. In this regard, normal Raman or RR spectroscopy is more feasible towards investigating environmental bacteria. To date, there is no report using single-cell Raman to study N_2-fixing bacteria in complex ecosystems. Identifying an indicative Raman band associated with N_2 fixation is the priority for the potential applicability of this approach.

Herein, we showed for the first time that $^{15}N_2$-induced shifts in the resonance Raman band of Cyt c are a sensitive and robust indicator of N_2-fixation. This biomarker was then used to discern and image the location of N_2-fixing bacteria in both artificial and complex soil communities at the single–cell level. The linear band shift *versus* $^{15}N_2$ percentages provided a good means to compare N_2 fixation extent of diverse soil bacteria. This work provides a novel single-cell resonance Raman approach to discern, image and compare fixation extent of N_2-fixing soil bacteria.

MATERIALS AND METHODS

Strains, media and growth conditions. Four model N_2-fixing bacteria, including two free-living *Azotobacter* sp. (AS1.222) and *Azotobacter chroococcum* (ACCC10096), two symbiotic *Rhizobium radiobacter* (ATCC15955) and *Bradyrhizobium japonicum* (ACCC15067), were purchased from Guangdong Culture Collection Center of Microbiology, China. *Azotobacter* sp. and *A.*

chroococcum were cultured in N-free azotobacter media containing 20 g L^{-1} mannitol, 0.2 g L^{-1} KH_2PO_4, 0.8 g L^{-1} K_2HPO_4, 0.2 g L^{-1} $MgSO_4 \cdot 7H_2O$, 0.1 g L^{-1} $CaSO_4 \cdot 2H_2O$, and trace amount of $Na_2MoO_4 \cdot 2H_2O$ and $FeCl_3$ at 28 ℃ and 180 rpm. *R. radiobacter* and non-N_2-fixing strain *Shewanella oneidensis* MR-1 were grown in Luria Bertani (LB) broth containing 10 g L^{-1} tryptone (Oxoid Ltd., England), 5 g L^{-1} yeast extract (Oxoid Ltd., England), and 10 g L^{-1} NaCl at 28 ℃ and 180 rpm. *B. japonicum* were grown in media containing 1 g L^{-1} yeast exact, 200 mL of soil extract and 10 g L^{-1} mannitol at 28 ℃ and 180 rpm. Unless otherwise stated, chemicals were purchased from Sinopharm Chemical Reagent Co., China.

Soil sample collection. Park soil samples were collected from grassland at a depth < 5 cm in the campus of Institute of Urban Environment, Xiamen, China (24°36′39.90″N 118°03′33.48″E). The soil samples were homogenized and sieved through a 0.6-mm sieve to remove small stones, grass roots and other debris, then stored at 4 ℃ prior to use.

Incubation of model N_2-fixing bacteria and soil microcosm with $^{15}N_2$ gas. An aliquot of 20 mL N-free azotobacter media was filled into a 40-mL crimp-top vial and then inoculated with 20 μL of *Azotobacter* sp. or *A. chroococcum* after 24-hour culture. Vials were sealed, and air in the headspace was replaced with mixture gas consisting of $^{15}N_2$ (99 atom%, purity >98.5%, Aladdin, China) and oxygen (volume ratio of N_2 to O_2 is 4:1) of different volumes to achieve $^{15}N_2$ of different percentages ($^{15}N_2/(^{15}N_2+^{14}N_2)$). Considering that ^{15}N content is 99% in commercial $^{15}N_2$ and 0.36% in natural abundance,[32] the final ^{15}N abundance relative to N_2 in air in the headspace was 99.36%, 49.68%, 25.02%, 10.22%, 0.36%, respectively. Bacteria incubated with different percentages of $^{15}N_2$ were harvested after culturing for 48 h. Soil microcosm contained 2 g of park soil in a 12 mL crimp-top vial. Vials were sealed, purged with

O_2 for 10 min to remove air and then replaced with appropriate volume of $^{15}N_2$ to achieve 80% $^{15}N_2$ and 20% oxygen in the headspace. The control soil microcosm was supplied with lab air. $^{15}N_2$-incubated soil microcosm and control were amended with 500 uL of 0.5 M glucose solution and incubated at room temperature (ca. 25 ℃) under low light conditions for 12 days. All of these incubations were performed in triplicate.

Extracting bacteria from soil microcosms by Nycodenz density gradient separation. Nycodenz density gradient separation was used to extract bacteria from soil. A modified protocol from a previous report was used.[17] Briefly, soils post-incubation were homogenized in 10 mL PBS (NaCl 8 g L^{-1}, KCl 0.2 g L^{-1}, Na_2HPO_4 1.44 g L^{-1}, KH_2PO_4 0.24 g L^{-1}) supplemented with 0.5% (v/v) Tween 20 (Aladdin) to detach soil particle-associated cells by vigorously vortexing for 30 min at room temperature. To separate bacteria from soil particles, 1 vol of the as-prepared soil slurries were introduced into an Eppendorf tube containing 1 vol of Nycodenz (≥98%, Aladdin) stock solution carefully. Nycodenz stock was prepared by dissolving 8 g of Nycodenz in 10 mL sterile water, producing a final density of 1.42 g·mL^{-1}. This density is proper for efficient capture of soil bacteria and separation from soil particles.[17,33] The tube was then centrifuged at 14000 g for 90 min at 4 ℃. The upper and middle aqueous layers containing bacteria were collected and mixed with 10 vol PBS in a fresh centrifuge tube. The bacteria inside were then collected by centrifuging at 5000 rpm for 10 min and washed with ultrapure water twice for further Raman analysis.

Single-cell Raman measurement and Raman mapping acquisition. To prepare bacteria for single-cell Raman measurements, bacterial solution from model strains or soil samples were washed twice by DI water by centrifuging at 5000 rpm for 3

min and then adjusting to a proper concentration in order to obtain single-cell dispersion on aluminum (Al) foil substrate.[34] An aliquot of 2 μL of the as-prepared bacteria were loaded on Al foil and air-dried at room temperature. To construct an artificial community consisting of *Azotobacter* sp. and *S. oneidensis*, one bacterial solution was applied to the Al foil and allowed to air-dry whereupon the second was applied to the same spot and also allowed to dry. Single-cell Raman spectra and Raman mapping were obtained using a LabRAM Aramis (HORIBA Jobin-Yvon) confocal micro-Raman system equipped with a 600 g/mm grating. Excitation was provided by a 532-nm Nd: YAG laser. A 100× dry objective with a numerical aperture of 0.9 (Olympus) was employed. For single-cell Raman measurements, acquisition time was 5 s and 25 spectra were acquired from each bacterial sample. Raman mapping was employed to generate Raman images of artificial communities and also soil bacterial community containing N_2-fixing bacteria. The step-size was set at 1.5 μm in a rectangular mapping area with acquisition time of 2 s on each point.

Raman spectral and mapping data analysis. LabSpec5 software (HORIBA Jobin-Yvon) was used to process single-cell Raman spectra. After spectral extraction and baseline subtraction (polynomial, degree 6), mean spectra from each sample were calculated. The overlapped 1114 (C-^{15}N) and 1129 cm^{-1} (C-^{14}N) bands were deconvoluted using the GaussLorenz peak fitting function and the resulting peak area was used to calculate the intensity ratio of these two bands. Principal component analysis (PCA) and the required spectral pre-processing were performed using IRootLab toolbox (https://code.google.com/p/irootlab/) running on MATLAB 2012a.[35,36] Spectral pre-processing included spectral extraction (from 1095 to 1145 cm^{-1}), rubberband subtraction and vector normalization. PCA was then performed by

reducing spectral variables to 10 factors accounting for more than 99% of the total variance. The resulting PCA 1-D (PC1) scores were plotted against $^{15}N_2$ percentages. OriginPro8.5 was used to perform statistical calculation of average value ± standard deviation and linear regression fitting. One-way ANOVA with Tukey's Multiple comparison test was conducted in GraphPad Prism 5 for significance analysis of ^{15}N-induced Raman band change; $P < 0.05$ was considered significant. Direct classical least square (DCLS) modelling in Labspec 5 was employed to construct a Raman image of N_2-fixing and non-N_2-fixing bacteria based on multidimensional Raman mapping data matrix. C-^{15}N band at 1114 cm^{-1} and C-^{14}N at 1129 cm^{-1} were selected as the model, and then DCLS operation finding the linear combination of model spectra that matched most closely the original data was applied to all traces of the original data sets to construct Raman image of each component.

Quantification of ^{15}N incorporation in N_2-fixing bacteria by isotope ratio mass spectroscopy (IRMS). To measure the bulk isotope composition (^{15}N %) of N_2-fixing bacteria incubated with different percentages of $^{15}N_2$ to natural N_2 in air, 0.01-0.05 mg (dry weight) of ^{15}N-labeled lyophilized bacteria and 0.15-0.18 mg of urea was placed in a tin capsule. For non labeled N_2-fixing bacteria, 1 mg of lyophilized cell powder was put in a tin capsule. Urea of 0.30-0.34 mg was used as standard. Samples were analyzed with an elemental analyzer (Flash HT 2000 Thermo Fisher) coupled via a ConFlo IV device to the IRMS (Delta V advantage). Isotope composition was calculated using the equation below:

$At^{15}N\% = (M_{urea} \times 46.67\% \times 0.367\% + M_{bacteria} \times 9.77\% \times {}^{15}N\%) / (M_{urea} \times 46.67\% + M_{bacteria} \times 9.77\%)$, where $At^{15}N\%$ is the percentage of ^{15}N in total N and can be measured by IRMS, M_{urea} and $M_{bacteria}$ are the weight of urea and bacteria in tin capsule, 0.367% is the natural abundance of ^{15}N in urea, 46.67% and 9.77% are the total nitrogen

content in urea and bacteria respectively, $^{15}N\%$ is the abundance of ^{15}N in bacteria that will be calculated.

RESULTS AND DISCUSSION

Resonance Raman spectra of cytochrome c is a common signal in diverse N_2-fixing bacteria.

To identify a common Raman signal in diverse N_2-fixing bacteria, we examined four model N_2-fixing bacteria including two rhizobium-originated (*B. Japonicum* and *R. radiobacter)* and two free-living *(Azotobacter* sp. and *A. chroococcum),* and five environmental N_2 fixers isolated from soil by plating soil slurry onto N-free agar plates. Only N_2-fixing bacteria can form colonies on these agar plates since atmospheric N_2 provided the sole nitrogen source required for their growth. These soil N_2-fixing isolates were affiliated to the genera of *Azotobacter*, *Rhizobium* and *Raoultella* based on 16S rRNA sequencing and phylogenetic analysis (Figure S1a). These genera were reported to be from N_2-fixer group.[9,37] To further confirm N_2 fixation potential of these strains, Dinitrogenase reductase genes (*nifH*), which are the most widely used marker gene to identity N_2-fixing bacteria, were amplified and visualized on agarose gel. All the model and soil N_2-fixer isolates displayed a band specific to *nifH* genes, which, however, are absent in non N_2-fixing *S. oneidensis*, *E.coli* and non-templated control (Figure 1a). Phylogenetic analysis of *nifH* amplicons further supported that these five soil isolates were N_2 fixers (Figure S1b).

Single-cell Raman spectra were acquired from four model N_2-fixing bacteria and all colonies (approximately 32) formed by N_2-fixing soil bacteria (Figure 1b). It is interesting to find that all of them display characteristic Raman bands of Cyt c at 749 cm^{-1} (pyrrole breathing mode), 1129 [ν(C-N)], 1312 [δ(C-H)], and 1589 cm^{-1} [ν(C-C)], which are almost the same as that of pure Cyt c. [21,38,39] Strong Cyt c signal

was also recently reported in symbiotic rhizobia isolated from legumes nodules.[40] These observations demonstrate that Cyt c is commonly present in both free-living and symbiotic N_2-fixing bacteria of either model or environmental strains. The existence of Cyt c in diazotrophs is associated with the crucial role of Cyt c in protecting respiration as a terminal oxidase by rapid consumption of O_2 affecting the activity of O_2-labile nitrogenase.[41] In addition, intensities of Cyt c relative to Amide I at 1664 cm^{-1} were found to fluctuate in these N_2-fixer. Both the physiological state of bacteria and the redox state of Cyt c were reported to affect Cyt c intensity. For instance, significantly higher Cyt c signal was observed in *Rhizobium leguminosarum* bv. *viciae* isolated from nodules than those grown in culture;[40] reduced state of Cyt c generated more intense signal than the oxidized state due to shift in electronic transition.[23] In addition, Raman signal of Cyt c is much stronger than that of other intracellular bacterial constituents, such as bands at 1002 cm^{-1} (phenylalanine), 1240 cm^{-1} (protein), 1450 cm^{-1} (lipid) and 1664 cm^{-1} (protein), despite their higher abundance. Cyt c is a hemeprotein showing maximum electronic absorption at around 550 nm,[42] matching well with the 532 nm laser and thus generating a selective resonance Raman enhancement.

Not only N_2-fixing bacteria show Cyt c RR peaks, RR signals of Cyt c have also been reported in nitrifier bacteria, annamonx bacteria, and electron-generating bacteria such as *S. oneidensis* (Figure 1b) and *Geobacter*.[21,23] Therefore, despite the fact that the strong and characteristic Raman signal of Cyt c makes it highly distinguishable, it is insufficient to identify N_2-fixing bacteria because Cyt c is also present in other bacteria that are unable to fix nitrogen. Among the four RR bands of Cyt c, the band at 1129 cm^{-1} was assigned to C-N stretch, providing a good potential

target to incorporate $^{15}N_2$ stable isotope into C-N. The resulting Raman shift would then provide additional evidence for N_2 fixation.

$^{15}N_2$-induced Raman shifts in cytochrome c are a biomarker of N_2-fixing bacteria

To test this hypothesis, we incubated *Azotobacter* sp. and *A. chroococcum* in N-free medium with different percentages of $^{15}N_2$ relative to N_2 in air, *i.e.*, 99.36%, 49.68%, 25.02%, 10.22% and 0.36% (^{15}N natural abundance). Mean single-cell Raman spectra from approximately 25 individual cells under each $^{15}N_2$ incubation conditions are shown in Figure 2a and 2b. It is notable to observe that the 1129 cm^{-1} band (C-N stretch) at 0.36% $^{15}N_2$ shifted markedly to 1114 cm^{-1} at 99.36% $^{15}N_2$. The around 15 cm^{-1} shift is very close to that the 13 cm^{-1} shift observed in ^{15}N isotopically labeled pure Cyt c,[43] confirming that it is the substitution of light ^{14}N with heavier ^{15}N in the C-N bond resulting in a decrease of vibrational frequency of C-N stretch. By comparison, no obvious shifts were observed in other Cyt c bands wherein N was absent: 749 cm^{-1} (ring breathing), 1312 cm^{-1} (C-H), 1589 cm^{-1} (C-C), or bacterial composition-related bands. Figure 2b shows the enlarged spectra including exclusively 1114 and 1129 cm^{-1} bands. With increasing $^{15}N_2$, the 1129 cm^{-1} band (C-^{14}N) decreased whilst the 1114 cm^{-1} band (C-^{15}N) increased. The co-existence of 1129 cm^{-1} and 1114 cm^{-1} in individual bacteria indicates that only a proportion of N in intracellular Cyt c is replaced by the heavier ^{15}N.

By deconvoluting these two bands using peak fitting in Labspec software (Figure S2), peak area ratio of 1114 cm^{-1} band against the sum of peak area of 1114 cm^{-1} and 1129 cm^{-1} bands ($Area_{1114}/(Area_{1114}+Area_{1129})$) from individual spectrum were plotted against $^{15}N_2$ percentages. A linear relationship with R^2 of 0.968 was obtained.

To achieve a rapid analysis of large numbers of spectra from single cells and avoid possible errors in deconvolution of overlapped spectra, PCA was also performed on spectral profile between 1095 and 1145 cm^{-1} (Figure 2c). Scores along PC1, accounting for 87.5% of variance, generated an even better linear relationship with $^{15}N_2$ percentages (R^2 = 0.998) than the peak area ratio (R^2 = 0.968).

To validate Raman results of N_2 fixation, bulk isotope analysis by isotope ratio mass spectroscopy was used to quantify how much N was fixed in bacteria. The abundance of ^{15}N in bacteria was determined to be 0.36% (close to natural abundance of ^{15}N), 5.89%, 15.01%, 29.97%, and 66.16%, and linearly increased with percentage of atmospheric incubation $^{15}N_2$ (Figure 2d), whereas non-N_2 fixer *S. oneidenis* containing Cyt c and *E. coli* only displayed ^{15}N of natural abundance. This measurement fully demonstrated that bacteria had incorporated ^{15}N and a higher $^{15}N_2$ percentage resulted in a higher incorporation extent and Raman shift. A further correlation analysis indicated that ^{15}N content of bacteria corresponded linearly to PC1 scores (Figure 2e), providing a way to measure the extent of N_2 fixation by RR spectral profile of Cyt c at single-cell level, protist.[16,44,45] ^{15}N abundance in bacteria was around three-fifth of the $^{15}N_2$ percentage, indicating that N_2 fixers were not fully labeled by ^{15}N, consistent with Raman result that both 1114 and 1129 cm^{-1} bands were observed. Detection limit of Raman-$^{15}N_2$ SIP was defined as the minimum $^{15}N_2$ that can induce significant spectral change. Spectral change was analyzed by PCA and the resulting PC1 scores were used for significance analysis of ^{15}N-induced spectral change via one-way ANOVA. Detection limit was determined to be 10.22% $^{15}N_2$, corresponding to 5.89% ^{15}N abundance in bacteria, at which spectra were significantly different from that in air (one-way ANOVA, $P < 0.05$). The linear band shifts were also obtained in *A. chroococcum* (Figure S3) with similar slope and

intercept (y = 0.098x - 0.5059) to that of *Azotobacter* sp. (y = 0.091x - 0.5411) based on PC1 scores.

Bacteria without Cyt c like *E. coli* display peaks at around 1123 cm^{-1} (carbohydrate), which is close to C-^{14}N and C-^{15}N at 1129 and 1114 cm^{-1} (Figure S4), but much lower, thus will not interfere ^{15}N-induced shift. Bacteria containing carotenoid show strong RR signal at 1155 and 1511 cm^{-1}. Although the band at 1155 cm^{-1} has some overlap with C-^{14}N band of Cyt c at 1129 cm^{-1}, it separates well with C-^{15}N band at 1114 cm^{-1}, thus exerting no effect on identification of $^{15}N_2$ fixation. Cyanobacteria can also fix N_2,[12] however, its fluorescence was too strong to observe Raman signal (Figure S5), so RR combined with $^{15}N_2$ is not enough to detect cyanobacteria as N_2 fixers. The further application of SERS with $^{15}N_2$ excited with a laser out of fluorescence can provide a solution.

The above observations indicate that the marked $^{15}N_2$-induced shift in C-N bond of Cyt c is a sensitive and highly distinguishable biomarker for N_2-fixing bacteria. The linear shift also provides a good means towards evaluating N_2-fixing extent in a quantitative manner.

Probing and Raman imaging of N_2-fixing bacteria in artificial communities

Important advantages of single-cell measurements lie in the ability to discern and image N_2-fixing bacteria in a complex community. Herein, an artificial community comprising *S. oneidensis* and $^{15}N_2$-incubated *Azotobacter* sp. was constructed. Both species contain Cyt c, while only *Azotobacter* sp. can fix nitrogen. Raman imaging was used to discern and locate $^{15}N_2$-fixing *Azotobacter* sp. in this artificial community.

343 Figure 3a shows a photomicrograph of such an artificial community with
344 *Azotobacter* sp. appearing as spherical and *S. oneidensis* as rod-shaped. Because of
345 their highly distinguishable shapes, the distribution of the two species is visually
346 relatively clear except when clumped on top of each other. By using the 1114 cm^{-1}
347 and 1129 cm^{-1} bands characteristic of ^{15}N-labeled N_2-fixing *Azotobacter* sp. and *S.*
348 *oneidensis* (^{14}N) respectively (Figure 3c), Raman imaging was acquired and
349 pseudo-color Raman image was generated (Figure 3b). Red regions were identified
350 as *Azotobacter* sp. whilst green regions as *S. oneidensis*. The distribution of both
351 bacterial species in Raman images is consistent with the conventional
352 photomicrographs. For example, the encircled spherical *Azotobacter* sp. in the
353 photomicrograph can be found in the same place as that shown in red in the
354 corresponding Raman image, as is the case for *S. oneidensis*. This result
355 demonstrates the accuracy of Raman imaging in indicating the site of N_2-fixing
356 bacteria. In addition, *Azotobacter* sp. that were clumped with *S. oneidensis* (labeled
357 with arrows) were hard to confirm their presence based on the photomicrographic
358 image (Figure 3a), but can be conclusively identified to be *Azotobacter* sp. based on
359 the red spot in the Raman image, demonstrating the potential of Raman imaging in
360 locating N_2-fixing cells in microbial communities.
361
362 **Probing and Raman imaging N_2-fixing bacteria of different activities in soil**
363 **communities**
364 We further applied $^{15}N_2$ incubation and Raman imaging to reveal N_2-fixing
365 bacteria in soil microbial communities. Soils harbor a multitude of our Earth's
366 biodiversity and also a high diversity of N_2-fixing bacteria in either free form or in
367 symbiosis with plants,[46] representing the main site wherein biological N_2 fixation is

naturally carried out. Herein, park soil was collected from a grassland that had been left fallow for a long period of time without application of fertilizer, providing a high probability of detecting N_2-fixing bacteria. Soil was placed in 12-ml vials filled with a mixture gas of $^{15}N_2$ (^{15}N 99.36%) and O_2 at volume ratio of 4:1. After a 12-day incubation, the soil samples were collected. To date, application of Raman spectroscopy for single-cell investigations in soil systems has been very limited,[17] because soil microorganisms are dispersed in a high background of soil particles. Separation of bacteria from soil particles is a necessity for either Raman or SIMS measurement.[17] Soil bacteria were detached from soil particles *via* gradient density centrifugation reported previously.[17] High-background soil particles can be largely reduced for both Raman and SIMS measurement. Figure 4 shows representative Raman spectra of individual soil bacteria with different phenotypes, including N_2-fixing bacteria identified by 1114 cm^{-1} (C-^{15}N) band (i), bacteria containing Cyt c but unable to fix N_2 (ii), bacteria containing Cyt c and carotenoid of different contents but unable to fix N_2 (iii, iv), as well as bacteria without any pigments (v). The above finding indicates a high diversity of bacteria with different phenotypes in soil.

Raman imaging was then applied to soil bacteria to discern and image N_2-fixing bacteria. Seven areas ranging from 20×20 to 30×30 μm^2 were mapped. Because of the high diversity of soil bacteria, not every area contained both N_2-fixer and non-N_2 fixer. Two areas containing both were shown in Figure 5. The photomicrograph (Figure 5a, 5b left) shows soil bacteria of different shapes and sizes, but provides no information on function. In contrast, we can use spectral profile covering 1114 cm^{-1} and 1129 cm^{-1} band (Figure 5c red and green) to discriminate N_2-fixing bacteria from non-N_2-fixing bacteria. The resulting Raman images clearly reveal that the red

dots are N_2-fixing bacteria (labelled as ^{15}N), and the green dots are non-N_2-fixing bacteria containing Cyt c (Figure 5a, 5b right). Encircled bacteria (labeled with 'no Cyt c' in Figure 5a) do not exhibit any pigment signal (Figure 5c, bottom curve labeled with 'no Cyt c') and thus appear as a dark point in the Raman image. Figure 5b shows photomicrographic and Raman images taken from another independent location. A total of six N_2-fixing bacteria were discerned in the two areas, including two (labelled as ^{15}N-2 and ^{15}N-3) in close contact with non-N_2-fixing bacteria. The green irregular shape connected with the ^{15}N-2 red dot shows good consistency with the photomicrographic image, indicating a sufficient spatial resolution in Raman images. These observations demonstrate that Raman images can discern N_2-fixing bacteria from soil communities based on their isotopic composition.

$^{15}N_2$-fixation extent by soil bacteria was also revealed based on spectral profile of C-^{15}N and C-^{14}N bands. Single-cell Raman spectra from a total of 29 individual N_2-fixing soil bacteria including the six identified above were incorporated together with the spectra of *Azotobacter* sp. incubated with different percentages of $^{15}N_2$ (Figure 2c). As a comparison, three Raman spectra from soil bacteria similar to *Azotobacter* sp. incubated with 0.36% $^{15}N_2$ were also incorporated; this clearly indicates the presence of non- or weak N_2-fixing bacteria in soil. PCA was then performed on spectra of N_2-fixer and non or weak N_2-fixer from soil to generate 1-D PCA scores (on the right of Figure 2c labeled as 'soil bacteria'). A larger variation in PC1 scores was observed in soil bacteria than *Azotobacter* sp. incubated with the same 99.36% $^{15}N_2$, indicating heterogeneous N_2-fixing extent from diverse soil bacteria. Based on the linear correlation between ^{15}N content measured by IRMS and PC1 scores of *Azotobacter* sp. incubated with different atmospheric $^{15}N_2$% (Figure 2e), ^{15}N content of soil bacteria were determined to be from 0 to 84.40 (on the right

of Figure 2e) by inputting PC1 scores of soil bacteria to the linear fitting equation of $^{15}N\%$ in cells = 38.79 + 75.18 × PC1. The even larger ^{15}N incorporation extent in most N_2-fixing soil bacteria than *Azotobacter* sp. should be related to the much longer incubation time of soil with $^{15}N_2$ (12 days) than *Azotobacter* sp. (2 days).

CONCLUSIONS

This is the first demonstration that single-cell resonance Raman spectroscopy with $^{15}N_2$-SIP can discern, image and compare the extent of N_2-fixation of diverse N_2-fixing bacteria in complex soil communities in a culture-independent fashion. Cyt c was demonstrated as a universal N_2-fixation biomarker by investigating both model and environmental strains screened from soils. Its strong resonance Raman signal, together with a remarkable ^{15}N-induced C-N band shifts of Cyt c, provided a robust biomarker to distinguish N_2-fixing bacteria from non-N_2-fixing bacteria with or without Cyt c. Raman imaging at micrometer resolution facilitated the location of N_2-fixing bacteria in both artificial and soil communities. The linear correlation of C-N band profile with $^{15}N_2$ percentages allowed a quantitative evaluation of N_2 fixation extent of diverse soil bacteria.

For future work, this single-cell resonance Raman-$^{15}N_2$ SIP approach can be applied to important N_2-fixing symbiont systems. The further combination with single-cell isolation and genome sequencing suitable for soil microorganisms will also be developed, in order to reveal the precise ecological role of largely unexplored uncultured diazotrophs (microbial dark matter) in diverse ecosystems.

References:

(1) Hoffman, B. M.; Lukoyanov, D.; Yang, Z. Y.; Dean, D. R.; Seefeldt, L. C. *Chem Rev* **2014**, *114*, 4041-4062.

(2) Cui, S. H.; Shi, Y. L.; Groffman, P. M.; Schlesinger, W. H.; Zhu, Y. G. *Proc. Natl. Acad. Sci. U. S. A.* **2013**, *110*, 2052-2057.
(3) Zehr, J. P.; Carpenter, E. J.; Villareal, T. A. *Trends Microbiol.* **2000**, *8*, 68-73.
(4) Shashar, N.; Cohen, Y.; Loya, Y.; Sar, N. *Mar Ecol Prog Ser* **1994**, *111*, 259-264.
(5) Rai, A. N.; Soderback, E.; Bergman, B. *New Phytol.* **2000**, *147*, 449-481.
(6) Lechene, C. P.; Luyten, Y.; McMahon, G.; Distel, D. L. *Science* **2007**, *317*, 1563-1566.
(7) Tai, V.; Carpenter, K. J.; Weber, P. K.; Nalepa, C. A.; Perlman, S. J.; Keeling, P. J. *Appl. Environ. Microbiol.* **2016**, *82*, 4682-4695.
(8) Ohkuma, M.; Noda, S.; Hattori, S.; Iida, T.; Yuki, M.; Starns, D.; Inoue, J.; Darby, A. C.; Hongoh, Y. *Proc. Natl. Acad. Sci. U. S. A.* **2015**, *112*, 10224-10230.
(9) Konig, S.; Gros, O.; Heiden, S. E.; Hinzke, T.; Thurmer, A.; Poehlein, A.; Meyer, S.; Vatin, M.; Mbeguie-A-Mbeguie, D.; Tocny, J.; Ponnudurai, R.; Daniel, R.; Becher, D.; Schweder, T.; Markert, S. *Nat Microbiol* **2016**, *2*, 16193.
(10) Woebken, D.; Burow, L. C.; Prufert-Bebout, L.; Bebout, B. M.; Hoehler, T. M.; Pett-Ridge, J.; Spormann, A. M.; Weber, P. K.; Singer, S. W. *ISME J.* **2012**, *6*, 1427-1439.
(11) Sohm, J. A.; Webb, E. A.; Capone, D. G. *Nat. Rev. Microbiol.* **2011**, *9*, 499-508.
(12) Woebken, D.; Burow, L. C.; Behnam, F.; Mayali, X.; Schintlmeister, A.; Fleming, E. D.; Prufert-Bebout, L.; Singer, S. W.; Corte´s, A. L. p.; Hoehler, T. M.; Pett-Ridge, J.; Spormann, A. M.; Wagner, M.; Weber, P. K.; Bebout, B. M. *ISME J.* **2015**, *9*, 485-496.
(13) Severin, I.; Stal, L. J. *FEMS Microbiol Ecol* **2010**, *73*, 55-67.
(14) Soares, R. A.; Roesch, L. F. W.; Zanatta, G.; Camargo, F. A. D.; Passaglia, L. M. P. *Appl Soil Ecol* **2006**, *33*, 221-234.
(15) Chalk, P. M.; He, J.-Z.; Peoples, M. B.; Chen, D. *Soil Biol. Biochem.* **2017**, *106*, 36-50.
(16) Roey Angel; Christopher Panhölzl; Raphael Gabriel; Craig Herbold; Wolfgang Wanek; Andreas Richter; Stephanie A. Eichorst; Woebken, D. *Environ. Microbiol.* **2018**, *20*, 44-61.
(17) Eichorst, S. A.; Strasser, F.; Woyke, T.; Schintlmeister, A.; Wagner, M.; Woebken, D. *FEMS Microbiol. Ecol.* **2015**, *91*, fiv106.
(18) Martinez-Perez, C.; Mohr, W.; Loscher, C. R.; Dekaezemacker, J.; Littmann, S.; Yilmaz, P.; Lehnen, N.; Fuchs, B. M.; Lavik, G.; Schmitz, R. A.; LaRoche, J.; Kuypers, M. M. *Nat Microbiol* **2016**, *1*, 16163
(19) Wang, Y.; Huang, W. E.; Cui, L.; Wagner, M. *Curr. Opin. Biotechnol.* **2016**, *41*, 34-42.
(20) Huang, W. E.; Griffiths, R. I.; Thompson, I. P.; Bailey, M. J.; Whiteley, A. S. *Anal. Chem.* **2004**, *76*, 4452-4458.
(21) Patzold, R.; Keuntje, M.; Theophile, K.; Muller, J.; Mielcarek, E.; Ngezahayo, A.; Ahlften, A. A. V. *J. Microbiol. Methods* **2008**, *72*, 241-248.
(22) Millo, D.; Harnisch, F.; Patil, S. A.; Ly, H. K.; Schroder, U.; Hildebrandt, P. *Angew. Chem. Int. Edit.* **2011**, *50*, 2625-2627.
(23) Virdis, B.; Harnisch, F.; Batstone, D. J.; Rabaey, K.; Donose, B. C. *Energ Environ Sci* **2012**, *5*, 7017-7024.
(24) Kubryk, P.; Kolschbach, J. S.; Marozava, S.; Lueders, T.; Meckenstock, R. U.; Niessner, R.; Ivleva, N. P. *Anal. Chem.* **2015**, *87*, 6622-6630.
(25) N., V. K. B.; Kampe, B.; Röschab, P.; Popp, J. *Analyst* **2015**, *140*, 4584-4593.
(26) Li, M. Q.; Canniffe, D. P.; Jackson, P. J.; Davison, P. A.; FitzGerald, S.; Dickman, M. J.; Burgess, J. G.; Hunter, C. N.; Huang, W. E. *ISME J.* **2012**, *6*, 875-885.
(27) Lutz, M. *J. Raman Spectrosc.* **1974**, *2*, 497-516.

(28) Berry, D.; Mader, E.; Lee, T. K.; Woebken, D.; Wang, Y.; Zhu, D.; Palatinszky, M.; Schintimeister, A.; Schmid, M. C.; Hanson, B. T.; Shterzer, N.; Mizrahi, I.; Rauch, I.; Decker, T.; Bocklitz, T.; Popp, J.; Gibson, C. M.; Fowler, P. W.; Huang, W. E.; Wagner, M. *Proc. Natl. Acad. Sci. U. S. A.* **2015**, *112*, E194-E203.
(29) Huang, W. E.; Stoecker, K.; Griffiths, R.; Newbold, L.; Daims, H.; Whiteley, A. S.; Wagner, M. *Environ. Microbiol.* **2007**, *9*, 1878-1889.
(30) Muhamadali, H.; Chisanga, M.; Subaihi, A.; Goodacre, R. *Anal. Chem.* **2015**, *87*, 4578-4586.
(31) Cui, L.; Yang, K.; Zhou, G.; Huang, W. E.; Zhu, Y. G. *Anal. Chem.* **2017**, *89*, 5793-5800.
(32) Mariotti, A. *Nature* **1983**, *303*, 685-687.
(33) Burmolle, M.; Hansen, L. H.; Oregaard, G.; Sorensen, S. J. *Microb Ecol* **2003**, *45*, 226-236.
(34) Cui, L.; Butler, H. J.; Martin-Hirsch, P. L.; Martin, F. L. *Anal Methods-Uk* **2016**, *8*, 481-487.
(35) Cui, L.; Zhang, Y.-J.; Huang, W. E.; Zhang, B.-F. M., Francis L; Li, J.-Y.; Zhang, K.-S.; Zhu, Y.-G. *Anal. Chem.* **2016**, *88*, 3164–3170.
(36) Zhang, B.; Cui, L.; Zhang, K. *Anal Bioanal Chem* **2016**, *408*, 3853-3865.
(37) Luo, T.; Ou-Yang, X. Q.; Yang, L. T.; Li, Y. R.; Song, X. P.; Zhang, G. M.; Gao, Y. J.; Duan, W. X.; An, Q. *J. Basic Microbiol.* **2016**, *56*, 934-940.
(38) Feng, C.; Li, J.; Qin, D.; Chen, L.; Zhao, F.; Chen, S.; Hu, H.; Yu, C. P. *Plos One* **2014**, *9*, e113379.
(39) Strekas, T. C.; Spiro, T. G. *Biochim. Biophys. Acta* **1972**, *278*, 188-192.
(40) Xu, J.; Webb, I.; Poole, P.; Huang, W. E. *Anal. Chem.* **2017**, *89*, 6336-6340.
(41) Poole, R. K.; Hill, S. *Biosci. Rep.* **1997**, *17*, 303-317.
(42) Droghetti, E.; Oellerich, S.; Hildebrandt, P.; Smulevich, G. *Biophys. J.* **2006**, *91*, 3022-3031.
(43) Hu, S. Z.; Morris, I. K.; Singh, J. P.; Smith, K. M.; Spiro, T. G. *J. Am. Chem. Soc.* **1993**, *115*, 12446-12458.
(44) Jochum, T.; Fastnacht, A.; Trumbore, S. E.; Popp, J.; Frosch, T. *Anal. Chem.* **2017**, *89*, 1117-1122.
(45) Keiner, R.; Herrmann, M.; Kusel, K.; Popp, J.; Frosch, T. *Anal. Chim. Acta* **2015**, *864*, 39-47.
(46) Paul, E. A. *Soil Microbiology, Ecology and Biochemistry*; Academic Press: Boston, 2014.

Supporting Information Available: Experimental description of 16s rRNA and *nifH* gene sequencing. Phylogenic trees. Deconvolution of Raman band and correlation of band area ratio with $^{15}N_2$ percentage. Raman spectra of other types of N_2-fixing bacteria and related bacteria.

Author information

Corresponding Author

*E-mail, ygzhu@rcees.ac.cn. Phone: 86-5926190997.

The authors declare no competing financial interest.

Acknowledgements

This work was supported by National Key Research and Development Program of China (2017YFD0200201, 2017YFE0107300), the Strategic Priority Research Program of Chinese Academy of Sciences (XDB15020302, XDB15020402), Natural Science Foundation of China (21777154) and K.C.Wong Education Foundation.

546 **Figure legends**

547 **Figure 1.** Gel image of PCR product of *nifH* genes specific for N_2 fixation (a) and
548 single-cell resonance Raman spectra (b) from N_2-fixing bacteria isolated from soil
549 (red), model N_2-fixing bacteria (blue), non N_2-fixing *S. oneidensis* and *E. coli* (black).
550 'No template control' in gel image is the negative control without DNA template for
551 PCR.

552 **Figure 2.** (a) Single-cell resonance Raman spectra of *Azotobacter* sp. incubated with
553 $^{15}N_2$ of 99.36%, 49.68%, 25.02%, 10.22%, 0.36% relative to N_2 in air. (b) Spectral
554 region including exclusively 1114 cm^{-1} (C-^{15}N) and 1129 cm^{-1} (C-^{14}N) bands
555 extracted from a. (c) Correlation between incubation $^{15}N_2$ percentage versus
556 ^{15}N-induced spectral changes in single cell based on PCA 1-D scores. Each point is a
557 measurement of a single cell, and around 25 cells were measured. (d) Quantification
558 of bulk ^{15}N content in *Azobacter* sp. from the same incubation as in Raman as
559 detected by isotope ratio mass spectroscopy. ^{15}N abundance in *E. coli* and *S.*
560 *oneidensis* incubated with 99.36% N_2 was also shown. (e) Correlation between ^{15}N
561 content of *Azobacter* sp (from d) and PC1 scores (from c). Data points on the right of
562 c and d labeled as soil bacteria were from active N_2-fixing and non or weak N_2-fixing
563 soil bacteria.

564 **Figure 3.** (a) Photomicrograph of a mixed artificial community containing N_2-fixing
565 *Azotobacter* sp. incubated with $^{15}N_2$ in N-free medium and non-N_2-fixing *S.*
566 *oneidensis* grown in LB medium - two images showing the different shapes
567 (isospherical vs. rod-shaped) of these two bacteria are shown below. (b)

568 Corresponding Raman image from the same area as in a. (c) Typical Raman spectra
569 acquired from *Azotobacter* sp. and *S. oneidensis* in a and b. Bands at 1114 cm^{-1}
570 (C-^{15}N) and 1129 cm^{-1} (C-^{14}N), representing $^{15}N_2$-fixing (red) and non-N_2-fixing
571 bacteria (green), were employed to construct the Raman image.

572 **Figure 4.** Single-cell Raman spectra of diverse soil bacteria extracted from soil after
573 12-day incubation with $^{15}N_2$. Each spectrum represents a characteristic phenotype. i,
574 N_2-fixing bacteria; ii, bacteria containing Cyt c but unable to fix N_2; iii and iv,
575 bacteria containing both Cyt c and carotenoid but unable to fix N_2; v, bacteria without
576 any pigment.

577 **Figure 5.** (a, b) Photomicrograph (left) and Raman images (right) of bacteria
578 extracted from soil microcosms incubated with $^{15}N_2$ for 12 days. (c) Resonance
579 Raman spectra of single cells from six N_2-fixing bacteria (^{15}N-1, 2, 3, 4, 5, 6),
580 non-N_2-fixing bacteria (^{14}N), and bacteria without Cyt c (no Cyt c) in a and b. Bands
581 at 1114 cm^{-1} (C-^{15}N) and 1129 cm^{-1} (C-^{14}N) were used to construct the Raman images
582 exhibiting N_2-fixing bacteria as red, non-N_2-fixing bacteria containing Cyt c as green,
583 and bacteria without Cyt c as black.

584

585

586

587

588

589

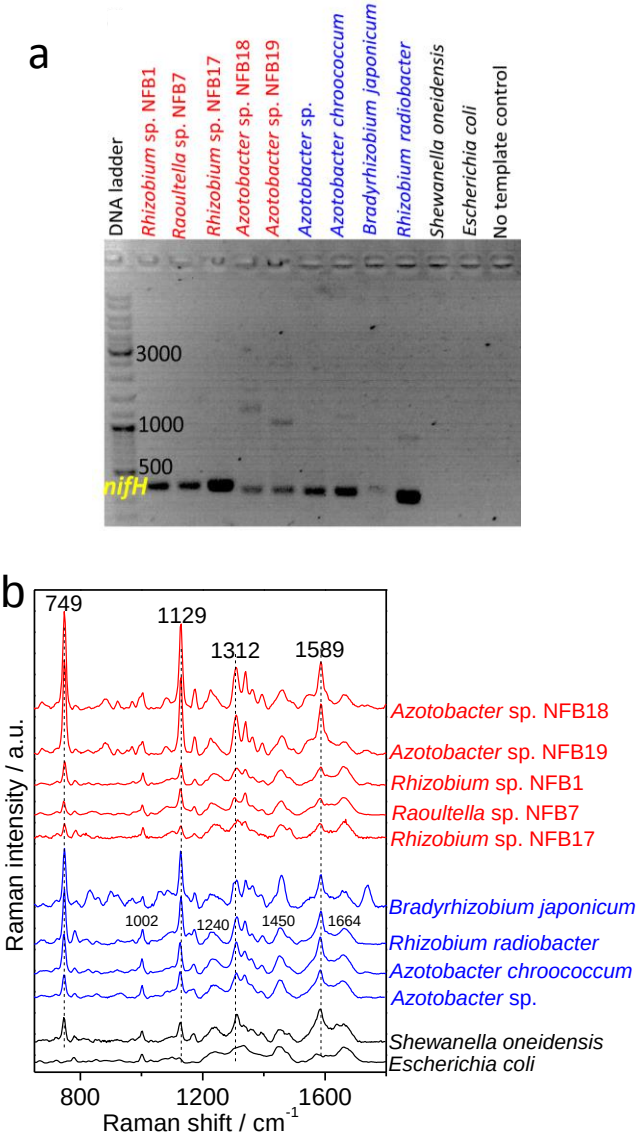
a
DNA ladder
Rhizobium sp. NFB1
Raoultella sp. NFB7
Rhizobium sp. NFB17
Azotobacter sp. NFB18
Azotobacter sp. NFB19
Azotobacter sp.
Azotobacter chroococcum
Bradyrhizobium japonicum
Rhizobium radiobacter
Shewanella oneidensis
Escherichia coli
No template control
3000
1000
500
nifH
b
749
1129
1312
1589
1002
1240
1450
1664
Azotobacter sp. NFB18
Azotobacter sp. NFB19
Rhizobium sp. NFB1
Raoultella sp. NFB7
Rhizobium sp. NFB17
Bradyrhizobium japonicum
Rhizobium radiobacter
Azotobacter chroococcum
Azotobacter sp.
Shewanella oneidensis
Escherichia coli
Raman intensity / a.u.
800
1200
1600
Raman shift / cm-1

Figure 1

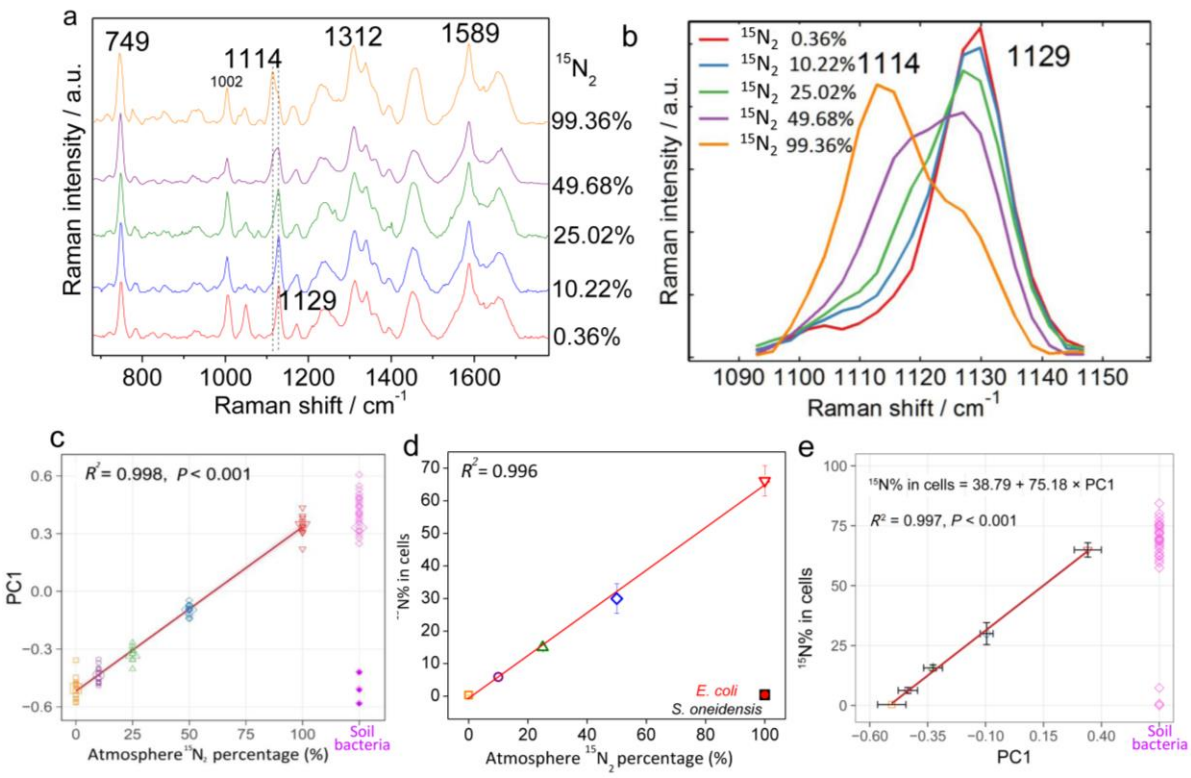
a
749
1114
1002
1312
1589
1129
$^{15}N_2$
99.36%
49.68%
25.02%
10.22%
0.36%
Raman intensity / a.u.
800 1000 1200 1400 1600
Raman shift / cm^{-1}
b
$^{15}N_2$ 0.36%
$^{15}N_2$ 10.22%
$^{15}N_2$ 25.02%
$^{15}N_2$ 49.68%
$^{15}N_2$ 99.36%
1114
1129
Raman intensity / a.u.
1090 1100 1110 1120 1130 1140 1150
Raman shift / cm^{-1}
c
R^2 = 0.998, P < 0.001
PC1
0.6
0.3
0.0
−0.3
−0.6
0 25 50 75 100
Soil bacteria
Atmosphere $^{15}N_2$ percentage (%)
d
R^2 = 0.996
^{15}N% in cells
70 60 50 40 30 20 10 0
0 20 40 60 80 100
E. coli
S. oneidensis
Atmosphere $^{15}N_2$ percentage (%)
e
^{15}N% in cells = 38.79 + 75.18 × PC1
R^2 = 0.997, P < 0.001
^{15}N% in cells
100 75 50 25 0
−0.60 −0.35 −0.10 0.15 0.40
Soil bacteria
PC1

Figure 2

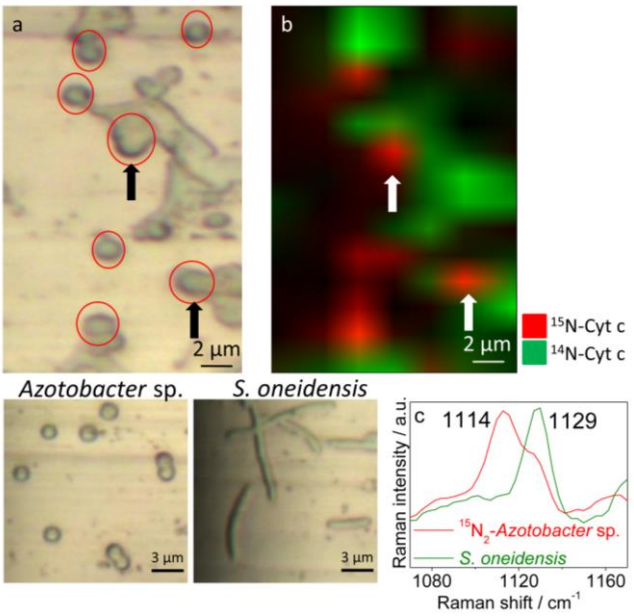

608

609 Figure 3

610

611

612

613

614

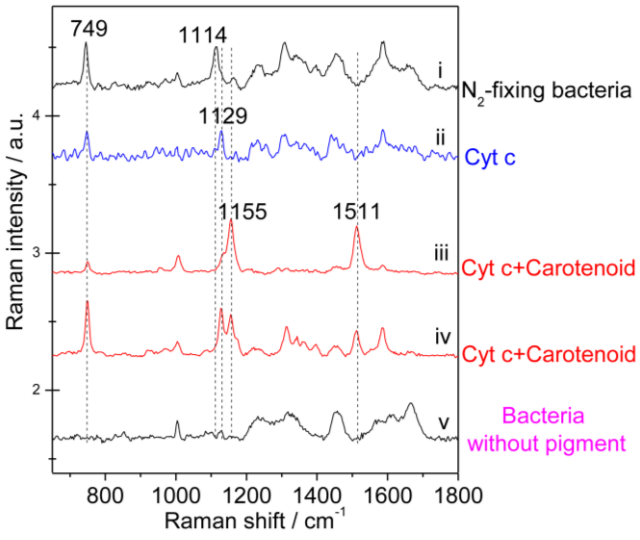

615

616 Figure 4

617

618

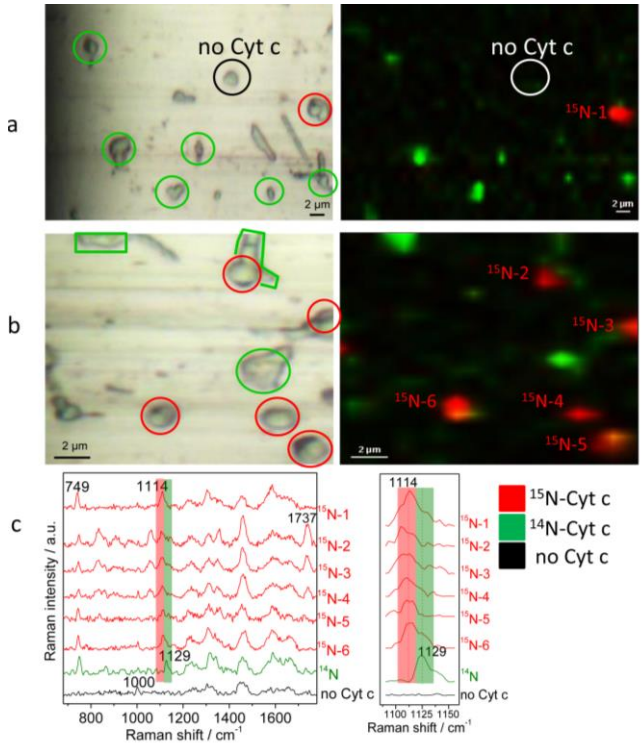

619

620 Figure 5